Cross-sectoral integration for increased penetration of renewable energy sources in the energy system – Unlocking the flexibility potential of maritime transport electrification

Mimica, Marko; Perčić, Maja; Vladimir, Nikola; Krajačić, Goran

Smart Energy 8 (2022) 100089

Contents lists available at ScienceDirect

Smart Energy

journal homepage: www.journals.elsevier.com/smart-energy

Cross-sectoral integration for increased penetration of renewable energy sources in the energy system – Unlocking the flexibility potential of maritime transport electrification

Marko Mimica [a,*], Maja Perčić [b], Nikola Vladimir [b], Goran Krajačić [a]

[a] Department of Energy, Power and Environmental Engineering, Faculty of Mechanical Engineering and Naval Architecture, University of Zagreb, Ivana Lučića 5, 10002, Zagreb, Croatia
[b] Department of Naval Architecture and Offshore Engineering, Faculty of Mechanical Engineering and Naval Architecture, University of Zagreb, Ivana Lučića 5, 10002, Zagreb, Croatia

A B S T R A C T

The creation of smart energy systems is essential for the energy transition of the European Union. Electrification and smart integration of maritime transport with the power system is becoming highly important in order to successfully decarbonise maritime transportation and increase the possibility for the integration of renewable energy sources. This study presents a novel method for the analysis of maritime transportation integration with the power system. The method includes a novel model for electric ships that include all relevant engine, ship route and energy storage system aspects. By including the ship charging variable it is possible to connect the model to the distribution grid. The method provides the possibility to analyse the impact of maritime integration for different connection options and with the different shares of renewable energy sources present in the system. The study found that such smart integration can have a positive impact on the overall smart energy system. In particular, the smart integration of maritime transport with the power grid led to the reduction of curtailed energy by 3.9 MWh in the Kvarner archipelago for the maximum analysed penetration of renewable energy sources.

1. Introduction

Environmental requirements regarding the Greenhouse Gases (GHGs) reduction forced the International Maritime Organization (IMO) towards setting an emission reduction target of 50% of annual GHG emissions from international shipping by 2050, compared to the 2008 levels [1]. According to the IMO decarbonization strategy, there are three levels of ambitions: short-term (2018–2023), mid-term (2023–2030) and long-term (2030-) ambitions. While the short-term ambitions refer to the beginning of GHGs reduction by tightening the Energy Efficiency Design Index (EEDI) or application of voluntary speed reduction, which results in lower fuel consumption and consequently significant GHGs reduction, the mid-term ambitions cover measures of the introduction of efficiency index for existing ships, i.e. Energy Efficiency Existing Ship Index (EEXI) [2], implementation of market-based measures and introduction of low-carbon fuels. The long-term ambitions focus on GHGs reduction up to 50% and higher, which is achievable with the development of innovative emission reduction technologies. Moreover, to achieve the ultimate GHGs reduction up to zero emissions from the international shipping sector by the end of this century, the development of zero-carbon fuels or carbon-neutral fuels is required [3]. These fuels, particularly hydrogen, ammonia, electricity, e-fuels, biofuels, etc., are investigated in a study by Korberg et al. [4] as advanced fuels for fossil-free ships, among which an electricity-powered ferry is highlighted as the most cost-effective option that offers zero-emission shipping, i.e. absence of tailpipe emissions during ship operation.

Although there are three different types of electrified ships, i.e. a hybrid ship, a plug-in hybrid ship and a full-electric ship, only the latter provide total elimination of the tailpipe emissions since it is powered by only energy storage [5]. Among different energy storage options, the implementation of a battery represents a better solution due to its high energy density and lower costs [6], where currently the most prominent battery for the maritime sector is Lithium-ion (Li-ion) battery [7]. Despite safe energy supply and mature technology, the main drawbacks of battery-powered ships are battery degradation, charging infrastructure and charging schedule [4]. Moreover, Gagatsi et al. [8] highlighted that the great disadvantage of the use of a battery for powering the ship is the limited range on which the ship can operate without recharging the battery. Battery-powered ships are currently only suitable for short-range routes in short-sea shipping, while the emission reduction for long-distance ships is achievable with other alternative low-carbon fuels [9]. However, with further development of metal-air batteries that have significantly higher energy density than a Li-ion battery [10],

* Corresponding author.
E-mail address: mmimica@fsb.hr (M. Mimica).

https://doi.org/10.1016/j.segy.2022.100089
Received 31 December 2021; Received in revised form 24 April 2022; Accepted 3 October 2022
Available online 11 October 2022

Nomenclature

Indices and sets

t	Time index
f	Ferry index
i,j	Node indexes
x	State of ship
k	Ferry route index
$\mathscr{T}$	Set of time periods
$\mathscr{N}$	Set of nodes
$\mathscr{F}$	Set of ferries
$\mathscr{E}$	Set of edges
$\mathscr{S}$	Set of nodes with photovoltaic power plants
$\mathscr{B}$	Set of nodes with energy storage systems
$\mathscr{K}$	Set of ferry routes

Parameters

$Q_f^{c,max}$	Maximum charging value of a ship f [MW]
ψ_f^{max}	Maximum state of charge of ship battery [MWh]
α, β	Battery parameters that define the minimum and maximum state of charge of ship battery
μ_f^c	The efficiency of ship charging
τ_f	Loss of battery charge coefficient
$E_{f,k}^d$	Discharging from ship battery during the navigation [MWh]
$v_{f,d}$	Designed speed for ship f [kn]
$v_{f,ave}$	The average speed of ship f [kn]
$P_{f,ave}$	Average ship f operating capacity [MW]
$P_{f,MEave}$	Average main engine capacity [MW]
$P_{f,AEave}$	Average auxiliary engine load [MW]
l_k	The length of the route k [nm]
EC_f	Average energy consumption of ship f per distance [MWh/nm]
λ_t	Price on the electricity day-ahead market [€/MWh]
CPV, $VOLL$	Penalty for the curtailed energy and lost load [€/MWh]
Z_{ij}	Impedance between nodes i and j [Ω]
θ_{ij}	Impedance angle between nodes i and j [rad]
$l_{i,t}^P, l_{i,t}^Q$	Active and reactive power load [MW], [MVar]
b	Line susceptance [μS]
V_{min}, V_{max}	Minimum and maximum voltage values [kV]
$\delta_{min}, \delta_{max}$	Minimum and maximum voltage angle [rad]
$\Lambda_{i,t}^{PV}$	Maximum available PV generation [MW]
η_c, η_d	Battery charging and discharging efficiency
SOC_i^{min}, SOC_i^{max}	Minimum and maximum battery state of charge [MWh]

Variables

$q_{i,t}^c$	Ship battery charging [MW]
$\psi_{f,t}$	Ship battery state of charge [MWh]
$p_{i,t}^{imp}, p_{i,t}^{eks}$	Active power import and export to/from the grid [MW]
$q_{i,t}^{imp}, q_{i,t}^{eks}$	Reactive power import and export to/from the grid [Mvar]
$p_{i,t}^{PV}, p_{i,t}^d, p_{i,t}^c$	Active power production from PV, energy storage discharge and charge [MW]
$q_{i,t}^{PV}, q_{i,t}^d, q_{i,t}^c$	Reactive power production from PV, energy storage discharge and charge [Mvar]
$s_{ij,t}$	Apparent power [MVA]
$p_{i,t}^{PVC}$	Curtailed power from PV plants [MW]
$ls_{i,t}$	Load shed [MW]
$p_{ij,t}, q_{ij,t}$	Active and reactive power flow [MW], [MVar]
$V_{i,t}$	Voltage at node i and time t [kV]
$\delta_{i,t}$	Voltage angle at node i [rad]
$i_{ij,t}$	Current through the line ij [A]
$soc_{i,t}$	State of the charge of the battery [MWh]
OF	Objective function

the full electrification of long-distance ships by using only a battery may be feasible.

The Life Cycle Assessment (LCA) has been widely used in many industries, as well as in the maritime industry [11]. Although battery-powered ships do not emit pernicious gases during navigation, when performing an environmental analysis of a ship, the main focus is put on the emissions generated by electricity production [12]. Perčić et al. [13] performed LCA and Life-Cycle Cost Assessment (LCCA) comparisons of nine different marine fuels implemented onboard three ferries operating in the Adriatic Sea and indicated that the battery-powered ship is the most environmentally friendly and cost-effective option among those investigated. Similar results are highlighted in a study by Wang et al. [14]. They performed LCA and LCCA comparisons of battery-powered catamaran ferry compared to the conventional ferry and indicated that fully electrification of the ship results in lower life-cycle GHG emissions and lifetime costs. The battery-powered ship is even more environmentally friendly when it is powered by electricity produced from RESs [13]. However, the available RESs in the coastal regions are often intermittent (solar, wind, waves) so special attention should be given to their integration into the new energy system. This is done by sector coupling and energy storage integrated into Smart energy systems. Sectors like electricity and transport were operated separately while increased electrification and development of digital technologies allowed their integration and optimisation in a new very complex and diverse environment. Smart energy systems must be supported by different platforms that will allow optimal energy and economy flows and business models for the flexibility provided by many new market players.

The analysis of energy systems has been widely conducted in the course of the previous two decades [15]. The importance of the energy planning models as decision support tools was emphasized in Ref. [16]. The EnergyPLAN tool was widely used for the smart energy system analysis as in Ref. [17] where the authors showed that there was no curtailed energy for the smart electrification scenario for the Madeira in comparison with the simple electrification scenario that had to curtail 7% of the production. The RenewIslands method was presented in Ref. [18] for analysing the effects of cross-sector integration on the islands. The approach presented in Ref. [19] analysed the microgrid operation with the availability of RES modelled as a chance constraint and found that the risk levels of not meeting (or exceeding) the energy demand higher than 30% did not correlate with additional microgrid benefits. The method for risk assessment of energy planning scenarios on islands was developed in Ref. [20], where the authors found that the zero import risk scenario for Unije island required a 3.5 MWh battery and a 0.5 MW PV plant. The tools for the meteorological forecasting that improve the energy planning process are also under development such as the FORCALM tool [21] demonstrated in the Sicily case.

The term flexibility is widely used by different authors in many recent studies in order to demonstrate the ability of smart energy systems to adapt their operation in order to reduce the cost of system operation [22]. Thus, the authors of the reported studies use the term flexibility to describe the energy management flexibilities of the system (e.g. inclusion of the battery system would increase the possibilities for energy management, thus would increase the flexibility of the energy system). However, the flexibility in the power systems is not related only to the energy, but also to the voltage flexibility, power or capacity

flexibility and the flexibility in transmission capacity import and export. For the distributions systems, voltage flexibility and energy management flexibility are relevant as the installed capacities and capacity import and export are insignificant with the respect to the transmission system. Although this is the case, the authors of the reported studies considered only energy management flexibility. This study analyses also the voltage flexibility with a focus on maritime transportation, which is an important research contribution.

The recent energy planning methods focused more on flexibility and the demand response as in Ref. [23], where the authors concluded that the investments in microgrid reduce by 10.9% as a result of demand response implementation. The presented methods and tools include the effects of the flexibility sources on the energy planning scenarios, however, they did not provide a detailed technical assessment and implementation possibilities of different flexibility solutions. The significant operational changes that occur as a result of the flexibility provision, especially from the large facilities (e.g. from industry facilities or maritime transportation as in this paper) can influence the conditions in the electric power grid. In this paper, the model that implemented relevant constraints imposed by the distribution system (e.g. voltage limits or power flow limits) was provided. This enabled the detailed evaluation of the electric and maritime sector integration, which was not previously done in the literature.

The study [24] showed that possible flexibility capacity as a result of a cross-sector integration is equal to 2.33 MW for the Krk island and 0.3 MW for the Vis island, however without specifying the contribution of maritime electrification to the systems' flexibility. Several studies proposed strategies for small islands decarbonization, such as [25] on the example of the island of Ustica, however without the consideration of maritime electrification. A similar study was conducted for Cyprus [26] where the results showed that installation of 3 kW rooftop PV on 50% of households would require additional 191 MW for covering the entire electricity demand. Another study [27] concluded that the transition from diesel-based to photovoltaics-battery diesel hybrid system of the Philippines off-grid energy systems can decrease the levelized cost of electricity by 20%. The road transport integration with other sectors was considered in Ref. [28] for the Caribbean island, with the conclusion that 78% of demand can be covered by RES with 1% of curtailed energy. The studies [15–27], however, did not include the electrification of the maritime transport and its integration with other sectors in their analysis. In this paper, this knowledge gap was filled by placing a focus on the maritime transport in the analysis of cross-sector integration.

To the best of the authors' knowledge, there is no method that used the proposed mathematical model for electrified maritime transport and simultaneously integrated it into the detailed distribution system model in order to assess the impacts and consequences of smart cross-sector integration of maritime transport and electric power system. The proposed method enables the observation of electric system operation variables such as voltage, losses, operation cost, curtailed energy, battery system operation as well as the operation and charging schedule of electric ships under different energy storage and RES penetration values. A novel electric ship model includes parameters regarding the ships' engine characteristics, route and energy storage system (ESS) specifications with charging variables modelled so that the model can be integrated into the distribution system. The importance of the proposed approach is in its ability to provide insight into the flexibility of energy as well as voltage while considering relevant ship and maritime parameters. The main contributions of the study are:

- A novel mathematical model for the electric ship operation
- An integrated model of electrified maritime transport with the electric distribution grid
- Sensitivity analysis for different RES penetration shares

The rest of the paper is organized as follows- After the Introduction, the Materials and methods section is presented. The third section presents the results of the study. The Discussion is presented in the fourth section. The final section is the Conclusion.

2. Materials and methods

2.1. General overview

This paper presents a novel method for the evaluation of smart cross-sector integration of electrified maritime transport and the electric power system. The method can be used for the comparison of different scenarios that include maritime electrification with the traditional electric power systems. Moreover, the method enables the evaluation of such cross-sector integration in a different environment (e.g. connection of the ESS with the electric chargers or assessment with respect to different RES penetration). The method is divided into two key parts:

- Defining the mathematical model of the electric ship
- Defining the mathematical model of the observed energy system and including the electric ship model in the energy system

The proposed method is illustrated in Fig. 1 and more detailly explained in the rest of the Materials and Methods chapter.

2.2. Electric ship mathematical model

Ships are designed to operate at certain speeds, i.e. design speeds ($v_{f,d}$), which corresponds to 70%–80% of the main engine load [29]. However, due to the rough weather conditions, strict operating schedule, voluntary speed reduction and others, the operating speed of a ship often differs from the design speed. The average operating speed of a ship ($v_{f,ave}$), can be calculated by dividing known route length by its duration. By considering the cubic relationship between ship speed and power, the average main engines capacity ($P_{f,MEave}$), is calculated with equation (1) [13].

$$P_{f,MEave} = \left(P_{f,ME} \bullet 0.8\right) \bullet \left(\frac{v_{f,ave}}{v_{f,d}}\right)^3 \tag{1}$$

The average auxiliary engines power is calculated with the assumption that the average load of these engines is 50%. The total average ship power ($P_{f,ave}$), is calculated with equation (2):

$$P_{f,ave} = P_{f,MEave} + P_{f,AEave} \tag{2}$$

The average energy consumption per distance, EC (kWh/nm), of an existing diesel-powered ship is calculated as follows (3):

$$EC_f = \frac{P_{f,ave}}{v_{f,ave}} \tag{3}$$

The energy consumption of a ship on a one-way route k is then described with equation (4).

$$E^d_{f,k} = EC_f \bullet l_k \tag{4}$$

The l_k represents the length of a route k, $\forall k \in \mathscr{K}$. The capacity of ships' battery storage needs to be sufficient enough to ensure the ship's navigation on a particular route. Therefore, the battery parameter – maximum state of charge (ψ_f^{max}) has to be chosen so that the ship has enough energy to navigate to the next charging station, respect the timeline and account for the safety margins that reduce the negative effects of battery degradation (denoted with α and β).

For every ship, there are three different states $x_{f,t} \in \{0,1,2\}, \forall f \in \mathscr{F}$, $\forall t \in \mathscr{T}$, where $x_{f,t} = 0$ is assigned to the ship in port and not charging, $x_{f,t} = 1$ to the ship in the port and charging and $x_{f,t} = 2$ for the ship $f \in \mathscr{F}$ that is sailing at time $t \in \mathscr{T}$. The full mathematical model of the electric ship can then be described with equations (5)–(7).

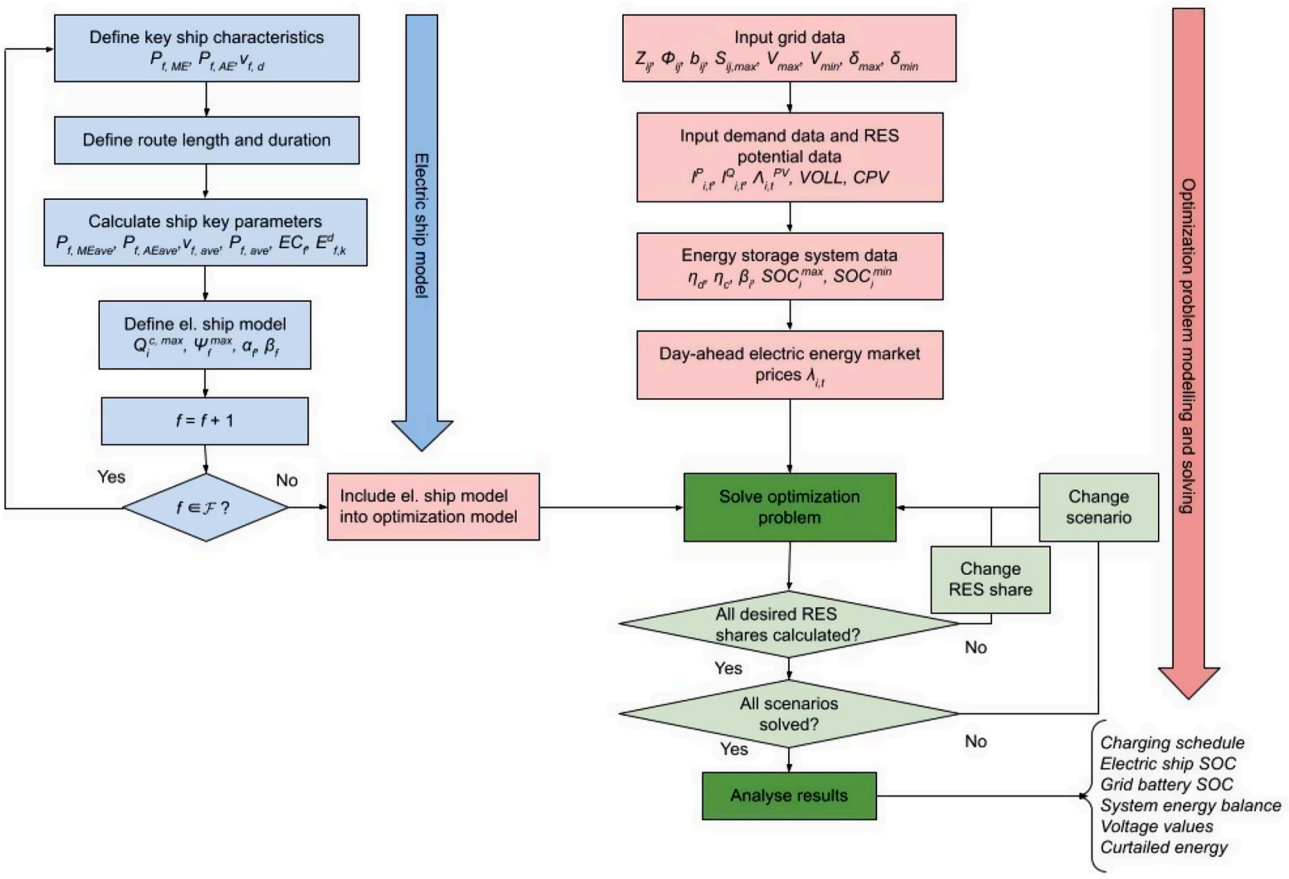

Fig. 1. The proposed method for evaluation of maritime electrification.

$$\psi_{f,t} = \begin{cases} (1-\tau_f)\,\psi_{f,t-1}, x_{f,t} = 0 \\ \psi_{f,t-1} + q^c_{i,t}\,\mu^c_{i,f}\Delta t, x_{f,t} = 1 \\ \psi_{f,t-1} - E^d_{f,k}, x_{f,t} = 2 \end{cases} \tag{5}$$

$$q^c_{i,t} \begin{cases} \le Q_i^{c,max}, x_{f,t} = 1 \\ = 0, else \end{cases} \tag{6}$$

$$\alpha_f\,\psi_f^{max} \le \psi_{f,t} \le \beta_f\,\psi_f^{max} \tag{7}$$

The state of charge of ships' battery ($\psi_{f,t}$) is given with equation (5) and is dependent on the current state of the ship ($x_{f,t}$). The energy loss of battery when the ship is in port is modelled with a coefficient (τ_f). When in the port ($x_{f,t} = 1$), the ship is charged on a charger i with charging power $q^c_{i,t}$ and efficiency of the ship charger $\mu^c_{i,f}$. The ships' energy consumption of ferry f, on the route k is described with $E^d_{f,k}$. This amount of energy ($E^d_{f,k}$) is reduced from the ship's battery during the sailing time of the ship ($x_{f,t} = 2$) which results in the decrease of the ship's battery state of charge ($\psi_{f,t}$). Equation (6) describes the charging capacity ($q^c_{i,t}$) that has to be less or equal to the maximum charging capacity ($Q_f^{c,max}$) for $x_{f,t} = 1$ and zero for other cases.

2.3. Mathematical model of the distribution system

The mathematical model used for the description of the energy system is a feasible non-linear optimisation problem. The model includes equations based on realistic constraints imposed by the distribution grid. The formed model is an NLP model solved in the GAMS tool with a CONOPT solver. The solver is suited for non-linear problems, especially effective for small-scale problems. Although the presented approach does not provide a solution with a global optimum, its results are sufficient for achieving the objectives of this paper, especially for the smaller distribution systems. The objective of the problem is to minimize the objective function *OF* defined in a manner described in equation (8).

$$minOF \triangleq min\left[\sum_{t\in\mathcal{T}}\sum_{i\in\mathcal{N}}\lambda_t\left(p^{imp}_{i,t} - p^{eks}_{i,t}\right) + CPV\sum_{t\in\mathcal{T}}\sum_{i\in\mathcal{N}}p^{PVC}_{i,t} + VOLL\sum_{t\in\mathcal{T}}\sum_{i\in\mathcal{N}}ls_{i,t}\right] \tag{8}$$

- Δt

Three types of costs are recognized in this method. The difference between the import and export ($p^{imp}_{i,t}$, $p^{eks}_{i,t}$) multiplied with the price on the day-ahead electricity market (λ_t) represents the first cost. Another cost is curtailed energy from RES ($p^{PVC}_{i,t}$) multiplied with a penalty for energy curtailment (CPV). Finally, the third cost is related to the lost load ($ls_{i,t}$) multiplied with the penalty or value of lost load (VOLL). The sum of these costs represents the overall cost of operation of the observed system.

The electric distribution grid constraints are introduced with equations (9)–(17). The constraints include a set of nodes and edges (lines or transformers). Afterwards, the renewable generation and the ESS are modelled (18)–(22) The input and output active and reactive power have to be equal at each node. This is modelled with equations (9) and (10), $\forall i \in \mathcal{N}$, $ij \in \mathcal{E}$, $\forall t \in \mathcal{T}$.

$$p^{imp}_{i,t} - p^{eks}_{i,t} + p^{PV}_{i,t} + p^{d}_{i,t} - p^{c}_{i,t} - l^{P}_{i,t} - q^{c}_{i,t} = \sum_j p_{ij,t} \tag{9}$$

$$q^{imp}_{i,t} - q^{eks}_{i,t} + q^{PV}_{i,t} + q^{d}_{i,t} - q^{c}_{i,t} - l^{Q}_{i,t} = \sum_j q_{ij,t} \tag{10}$$

The active power flow over between two nodes $ij \in \mathscr{E}$ is defined with the voltage at the beginning and the end of the line as well as the impedance of the line as in equation (11), $\forall ij \in \mathscr{E}, \forall t \in \mathscr{T}$. The active power flow is calculated as a squared voltage at the beginning node divided by the impedance minus the multiplication of beginning and end node voltage divided by the impedance. The expressions have to be multiplied by trigonometric function cosine because the active power ($p_{ij,t}$) represents a real part of the apparent power ($s_{ij,t}$). In addition to the parameters in (11), the reactive power flow is also defined with the susceptance as in equation (12), $\forall ij \in \mathscr{E}$, $\forall t \in \mathscr{T}$. Since the reactive power represent the imaginary part of the apparent power the expressions have to be multiplied by the sinus trigonometric function. The expression with susceptance (b) has to be also included in (12) because of the capacitive contributions of the lines.

$$p_{ij,t} = \frac{V_{i,t}^2}{Z_{ij}} \cos\left(\theta_{ij}\right) - \frac{V_{i,t} V_{j,t}}{Z_{ij}} \cos\left(\delta_{i,t} - \delta_{j,t} + \theta_{ij}\right) \tag{11}$$

$$q_{ij,t} = \frac{V_{i,t}^2}{Z_{ij}} \sin\left(\theta_{ij}\right) - \frac{V_{i,t} V_{j,t}}{Z_{ij}} \sin\left(\delta_{i,t} - \delta_{j,t} + \theta_{ij}\right) - \frac{b V_{i,t}^2}{2} \tag{12}$$

The apparent power flow between the two nodes is defined as a product of voltage and a complex conjugate of the current as in equation (13). Upper and lower values of the apparent power are defined with equation (14). Finally, the current ($i_{ij,t}$) between the nodes i and j is defined with equation (15). The current is defined as the voltage difference between nodes i and j divided by the impedance between i and j with added capacitive currents defined by the susceptance (b). It should be noted that $s_{ij,t} \neq s_{ji,t}$, $\forall ij \in \mathscr{E}$, $\forall t \in \mathscr{T}$, and the difference between these two variables represent the losses of the system.

$$s_{ij,t} = \left(V_{i,t} \angle \delta_{i,t}\right) i_{ij,t}^{*} \tag{13}$$

$$-S_{ij,max} < s_{ij,t} < S_{ij,max} \tag{14}$$

$$i_{ij,t} = \frac{V_{i,t} \angle \delta_{i,t} - V_{j,t} \angle \delta_{j,t}}{Z_{ij} \angle \theta_{ij}} + \frac{b V_{i,t}}{2} \angle \left(\delta_{i,t} + \frac{\pi}{2}\right) \tag{15}$$

The minimum and maximum voltage values are given with equation (16), $\forall i \in \mathscr{N}, \forall t \in \mathscr{T}$, while the maximum voltage angle difference between the two nodes is given with (17), $\forall ij \in \mathscr{E}, \forall t \in \mathscr{T}$.

$$V_{min} \leq V_{i,t} \leq V_{max} \tag{16}$$

$$\delta_{min} \leq \delta_{ij,t} \leq \delta_{max} \tag{17}$$

The sum of produced energy and curtailed energy from the PV has to be equal to the overall production potential of the production from PV as in equation (18), $\forall i \in \mathscr{S}, \forall t \in \mathscr{T}$.

$$p_{i,t}^{PV} + p_{i,t}^{CPV} = \Lambda_{i,t}^{PV} \tag{18}$$

The mathematical model of the ESS is given with equations (19)–(22), $\forall i \in \mathscr{B}$, $\forall t \in \mathscr{T}$. Equation (19) models the state of charge of the battery system. Maximum and minimum states of charge values are given with equation (20). Finally, maximum values of charging and discharging power of the ESS are given with equation (22).

$$soc_{i,t} = soc_{i,t-1} + \left(p_{i,t}^{c} \eta_c - \frac{p_{i,t}^{d}}{\eta_d}\right) \bullet \Delta t \tag{19}$$

$$SOC_i^{min} \leq soc_{i,t} \leq SOC_i^{max} \tag{20}$$

$$p_{i,t}^{c} \Delta t \leq \beta_i SOC_i^{max}, \beta_i \in [0, 1] \tag{21}$$

$$p_{i,t}^{d} \Delta t \leq \beta_i SOC_i^{max}, \beta_i \in [0, 1] \tag{22}$$

3. Case study

The case study in this research was conducted on the example of the Kvarner archipelago. The electrification of two Croatian ferries that operate on ferry line Valbiska-Merag, which connects the island of Krk with the island of Cres was investigated in this paper. The route length is 3.62 nm, while its duration is 25 min [30]. The ship specifications are obtained from the Croatian Register of Shipping [31] and presented in Table 1.

The observed electric power system is part of both the transmission and the distribution system (Fig. 2). It is characterised by two main substations Krk 110/35 kV (between bus 1 and 2) connected to the mainland and Lošinj 110/35/10.5 kV (three winding between bus 12 and 13). A 110 kV line is connecting these two substations. On the lower voltage side of these transformers, a distribution system is connected. The 1 MW PV plant and 0.4MW/1.6 MWh ESS are connected on the island of Unije (bus 23). Additionally, a 6.5 MW PV plant Orlec is installed at bus 7. This is considered to be a base case scenario (later noted as a 25% RES scenario).

The demand and PV production as well as the data about grid elements were obtained from Ref. [33] (Table 2 and Table 3). The day-ahead market prices are available from the Croatian day-ahead market [34]. The elements of the system are modelled with detailed electrical parameters that include resistance, reactance, susceptance, voltage, types of windings and nominal capacities. The per-unit method [pu] was used for the expression of system characteristics in order to avoid changes in system characteristics when referred from one side of the transformer to another (different voltage levels). The rest of the parameters used in the case study are provided in Table 4.

The power system is characterised by two specific periods of operation – during minimum and maximum demand. The input data about the reference voltage at node 1 were taken from the measurements from the Krk substation [32]. The measurements indicate that system can operate normally during maximum demand, however, during minimum demand, the reference voltage at node 1 was higher, thus indicating the possible grid code violations during the period of minimum demand and high RES production. For this reason, all modelled scenarios were analysed for a day of operation for these two cases, which is detailly discussed in the Results as well as the Discussion section. The demand data for minimum and maximum case is provided in Fig. 3. The system is analysed on for half – hourly periods.

Finally, three different scenarios were analysed in this study and are presented in Table 5.

For both scenarios, S1 and S2, it was considered that ships Krk and Kornati were electrified and that both ships are equipped each with a 2.4MW/1.2 MWh battery system. The batteries of such capacities are sufficient to follow the ships' timeline for winter and summer provided in Table 6. Merag port is located at node 4 and Valbiska in nearby node 2 in Fig. 2. It was considered that the Krk ship (F1) started at Merag port and the Kornati ship (F2) started at Valbiska port.

The connection of charging infrastructure for electric ships requires a large intervention in the existing power system grid. This requires the installation of additional transformers, cables and additional electric equipment. Moreover, since the charging capacity is high, significant

Table 1
Ship specifications.

Ship's name	Kornati	Krk
Length between perpendiculars (m)	89.1	89.1
Breadth (m)	17.5	17.5
Draught (m)	2.40	2.40
Main engine(s) power, P_{ME} (kW)	1764	1764
Auxiliary engine(s) power, P_{AE} (kW)	840	1080
Design speed, v_{de} (knot)	12.3	12.3
Passenger capacity	616	616
Vehicle capacity	145	145

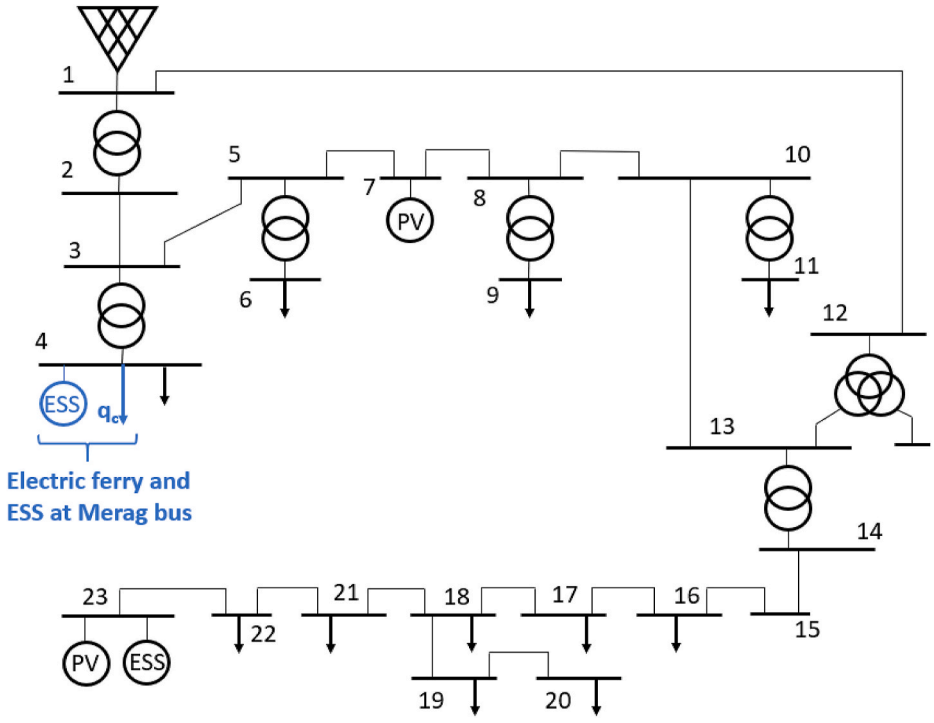

Fig. 2. Scheme of the electric power system of the Kvarner archipelago.

Table 2
Data about the lines in the system.

i	*j*	Type	Length (km)	Voltage [kV]
2	3	Cu 3x150	10	35
3	5	Cu 3x50	15.64	35
1	12	AlĆ 3x150	65	110
5	7	Cu 3x50	7	35
7	8	Cu 3x50	10	35
8	10	Cu 3x50	13.511	35
10	13	Cu 3x50	13.752	35
14	15	XHE 49-A 3x(1x185)	0.595	10
15	16	XHE 49-A 3x(1x150)	0.41	10
16	17	XHE 49-A 3x(1x150)	2.42	10
17	18	XHE 49-A 3x(1x185)[a]	5.567	10
18	19	RGS5H-10 JF 3x70	6.931	10
19	20	XHP 48-A 3x(1x95)	0.61	10
18	21	RGS5H-10 JF 3x70	3.024	10
21	22	RGS5H-10 JF 3x70[a]	7.353	10
22	23	XHE 49-A 3x(1x185)	1.2	10

[a] Consisted of more line types, the longest one is taken.

Table 3
Transformer data in the observed grid.

i	*j*	$u_{k\%}$	Type	Nominal capacity [MVA]
1	2	9	Yd5	8
3	4	4	Yd5	4
5	6	5.8	Yd5	8
8	9	5.8	Yd5	8
10	11	5.8	Yd5	8
12	13	11	YNyn0d5[a]	20
13	14	5.8	Dyn5	2.5

[a] Three-winding transformer.

energy electronic equipment needs to be installed which can negatively affect the quality of electric energy. A significant number of ships operate on 60 Hz frequency, which can require additional electronic devices such as frequency converters. More types of connection is provided in the study [35]. In this study, it is considered that the Merag transformer was upgraded from 35/0.4 kV to 35/10 kV and that the connection of electrical chargers is on the 10 kV voltage.

Four scenarios with different RES shares were analysed in this study

Table 4
Parameters used in the case study.

Parameter	Value
η_d, η_c	0.95
μ^c	0.95
α	0.1
β	0.9
τ_f	0
CPV	150 €/MWh
VOLL	3000 €/MWh

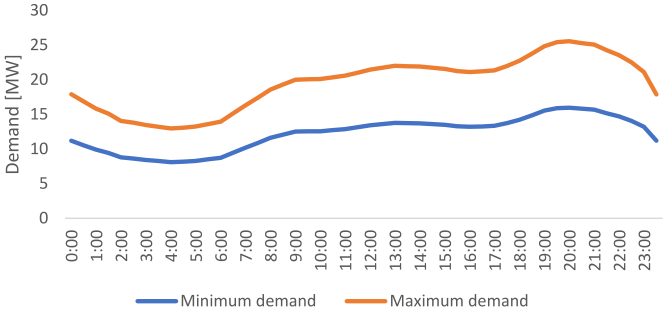

Fig. 3. The demand for two analysed days.

Table 5
Description of modelled scenarios.

Scenario	S0	S1	S2
Description	No maritime electrification	Maritime transport electrification with 2.4 MW charger in node 4	S1 + connection of 1MW/2 MWh ESS in node 4

Table 6
Timeline for Krk and Kornati ship for winter and summer periods.

Winter		Summer	
Merag →	Valbiska ←	Merag →	Valbiska ←
05:30	05:00	05:00	05:30
07:00	06:30	06:30	07:00
09:00	08:30	08:30	09:00
10:30	10:00	10:00	10:30
13:00	12:30	11:30	12:00
15:30	15:00	13:00	13:30
18:00	17:30	14:30	15:00
20:00	19:30	16:00	16:30
22:00	21:30	17:30	18:00
23:30	23:00	19:00	19:30
		20:30	21:00
		22:00	22:30
		23:30	

for each scenario (S0, S1 and S2), as well as minimum and maximum electricity demand (this corresponds to the winter and summer timeline of ships, respectively). The 25% RES scenario indicates the scenario with a total of 7.5 MW PV installed, while the 100% RES scenario is the scenario with 30 MW installed PV plants. Detailed connection points of added residential and utility PV plants are given in Table 7.

4. Results

The results were observed for two base cases – maximum and minimum demand. The positive effects of smart sector integration are visible in both cases, however, the positive effects are more expressed for the minimum demand case due to the aggravated technical conditions in the electric grid. The results present the differences in the charging schedule of the electric ships, operation of the ESS, voltage values, curtailed energy values and the overall system operation for different scenarios and different RES shares.

The results regarding ship dimensioning are presented in Table 8. These results were obtained based on the data in Table 1 and equations (1)–(4) presented in the Methods section.

4.1. Maximum demand

The operation of both electric ships – Krk (F1) and Kornati (F2) for scenarios without (S1) and with (S2) ESS in node 4 is presented in Figs. 4 and 5. Fig. 4 presents the charging of both electric ships at chargers installed at node 4. Both scenarios are presented in Fig. 4 since the installation of the ESS in node 4 did not change the charging schedule of both electric ships. The charging schedule, however, did slightly change for different RES shares (e.g., charging of the Kornati ship increased by 0.3 MW at 9:00 for 100% RES in comparison to 25% RES). The blue arrows in Fig. 4 point to the changes in the charging schedule for the first ship Krk (F1) and the red arrows point to the changes for the second ship Kornati (F2).

The charging schedule of the ships provides flexibility to the system so that it minimizes the operation cost. However, the system can exploit the flexibility only for a few periods because the charging schedule of the ships is primarily determined by the ship's navigation schedule. The installation of ESS in node 4 (S2 scenario) did not cause additional changes in the charging schedule of the ships because the battery provided additional flexibility during other periods when ship batteries were not able to provide it (see Fig. 6). Similarly, the state of charge of the ships' batteries remains similar with slight changes caused by the penetration of different RES shares in the system (Fig. 5).

Table 7
Connection of PV generation for different RES share.

Node	25% RES [MW]	50% RES [MW]	75% RES [MW]	100% RES [MW]
7	6.5	9	9	9
10	0	0	0	5
12	0	0	7.5	10
13	0	5	5	5
23	1	1	1	1
Total	**7.5**	**15**	**22.5**	**30**

Table 8
Parameters for Krk and Kornati ship.

Ship's name	Kornati	Krk
Average speed, v_{ave} (knot)	8.68	
Average main engine(s) power, $P_{ME,ave}$ (kW)	496.35	
Average auxiliary engine(s) power, $P_{AE,ave}$ (kW)	420	540
Total average ship power, P_{ave} (kW)	916.3	1036.3
Energy consumption per distance, EC (kWh/nm)	105.57	119.39

The operation of the ESS connected in node 4 (S2 scenario) is presented in Fig. 6. The ESS did not change its operation as the RES share in the system increased. This result was expected because the system operates at a stable voltage for all scenarios. Because of that, the operation of the battery is only determined by the demand curve and the day-ahead electricity market prices. The battery charged during the night hours and low market prices and it increased during the evening and higher market prices.

Fig. 7 presents the changes in the voltage at node 4 for different RES shares and all three scenarios. It can be seen that the increase in RES share caused the voltage level to increase as well. However, this did not impose significant constraints for the system operation because the voltage did not significantly approach the limits prescribed by the grid code. Another observation from Fig. 4 regarding the maritime electrification effect and RES integration can be derived. It can be seen that the electrification of maritime transport (green and red lines in Fig. 7) had a positive effect on the technical conditions in the grid. During the periods of ship charging, the voltage at node 4 reduced and brought it closer to the nominal voltage (1 pu). The impact of the ESS connection at node 4 (green line) decreased the voltage during charging periods and increased during the discharging periods. However, the operation of the ESS and ship charging for the maximum demand case is primarily determined in a way that they decrease the overall system operation cost, but they also provide additional flexibility in technical terms so that there is a higher potential for the RES integration in the system. The lowest voltage value for the 100% RES S2 scenario was 0.98 pu, while the highest was 1.07 pu.

The energy system operation for the S3 scenario and for the maximum demand case is presented in Fig. 8. The figure shows the impact on the overall energy exchange as a result of ship charging and installed ESS. As shown in the figure, there were no curtailed energy values for the maximum demand case.

It is important to note that during the maximum demand there are no significant challenges to maintaining the system parameters within the limits prescribed by the grid code. This is why the flexibility provided by the ship charging stations and the installed ESS was not necessary for preventing violation of technical limits of the energy system but was used for decreasing the operation cost of the system, thus increasing overall social welfare. This will, however, change for the case with minimum demand as the voltage limits will rise closer to the upper limit (1.1 pu) because of increased reactive power flows.

4.2. Minimum demand

The case with minimum demand is characterised by high voltage, caused by the increased reactive power flow in the distribution and transmission grid. Increased RES share in such conditions can further aggravate the voltage conditions in the observed grid. However, the results indicate that enabling flexibility through smart cross-sectoral integration of maritime transport with the electric power system grid

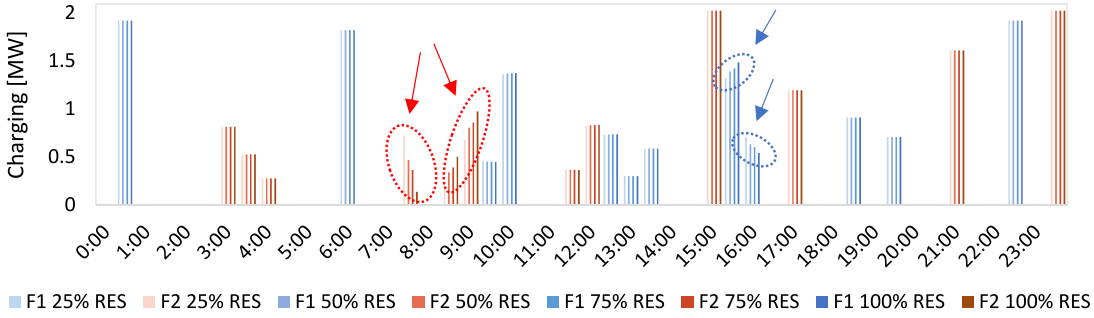

Fig. 4. Ship charging values for scenarios S1 and S2 (without and with the ESS in node 4) – first ship Krk (F1) in blue columns and the second one Kornati (F2) in red columns. (For interpretation of the references to colour in this figure legend, the reader is referred to the Web version of this article.)

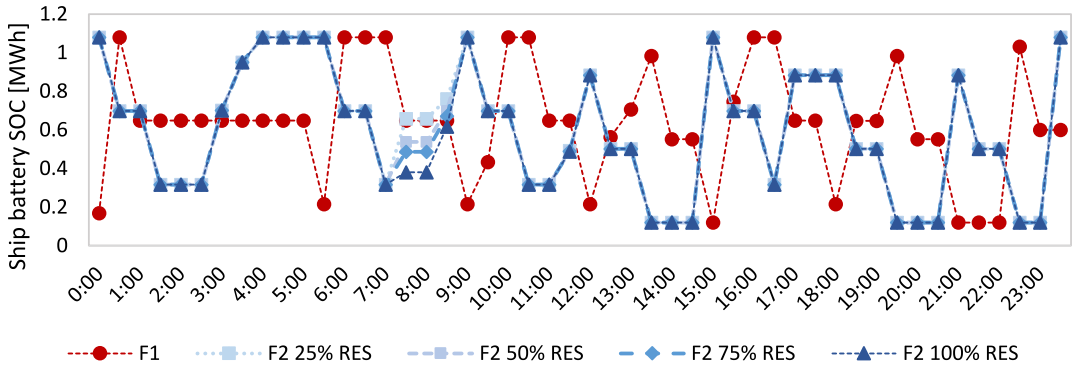

Fig. 5. State of charge of the ferry batteries for scenarios S1 and S2 (without and with the ESS in node 4).

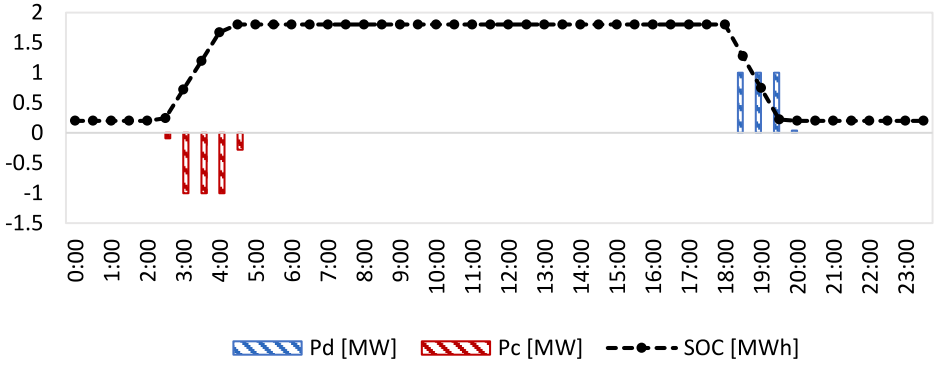

Fig. 6. Battery operation at node 4 for scenario S3.

can improve the conditions, lower the curtailed energy from the RES and enable higher RES penetration.

Figs. 9 and 10 present the operation of the Krk and Kornati charging schedule for scenarios S1 and S2. In contrast to the case for the maximum demand, significantly more changes in the charging schedule for different RES shares occurred. In particular, the changes are most evident for the cases when RES share reaches 75% and 100%. This result was expected, because high RES penetration increased the system voltage, bringing it closer to prescribed limits (1.1 pu) on specific buses. This leads to the curtailment of renewable energy and, in order to reduce the curtailed energy, the electric ships can provide flexibility to the extent possible so that the navigation schedule is respected. The results showed the necessity to invest in smart energy systems to integrate a large amount of RES.

Moreover, the results showed the difference in charging schedule between scenarios S1 and S2 as well. For example, the charging of the Krk ship (F1) was reduced by 10% at 13:00 for the 100% RES S3 scenario with the ESS in comparison to the S1 scenario (black arrow in Fig. 9). Similarly, the charging for the Kornati ship was reduced by 7.4% at 15:30 for the same scenario comparison (Fig. 10). More expressed changes for the Kornati ship can also be observed in Fig. 10. For example, a 2.02 MW charging was scheduled at 10:30 only for the 100% RES S2 scenario and a 1.61 MW at 14:30 for the same scenario (noted with black arrows in Fig. 10). It is interesting to observe that these changes are in line with the battery system operation for the S2 scenario shown in Fig. 12 (e.g., ESS discharged at 10:30 and 14:30 when the ships charged and ESS charged at 15:30 when the charging of the Kornati ship was reduced).

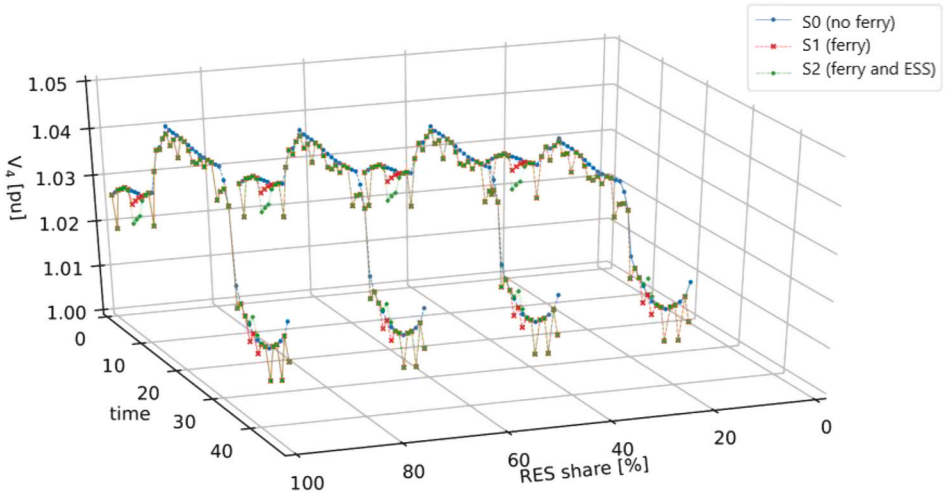

Fig. 7. The voltage at node 4 for all three scenarios for maximum demand.

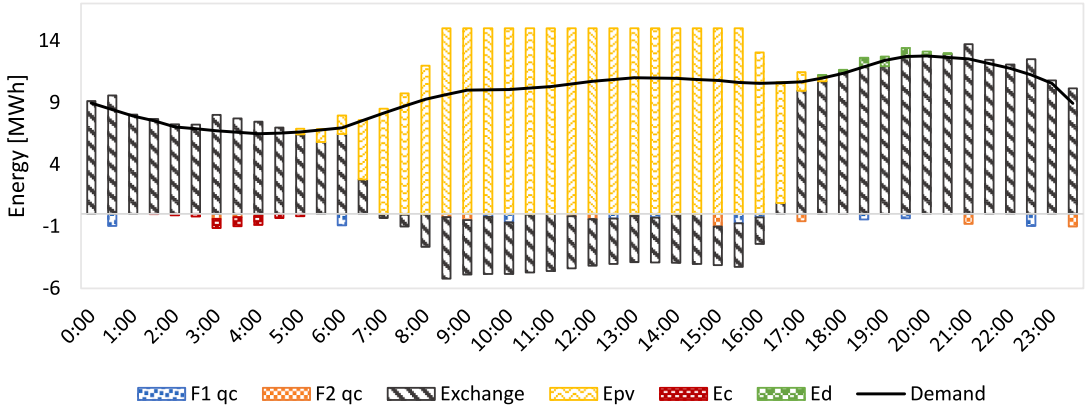

Fig. 8. Energy system operation for scenario S2 for the maximum demand case.

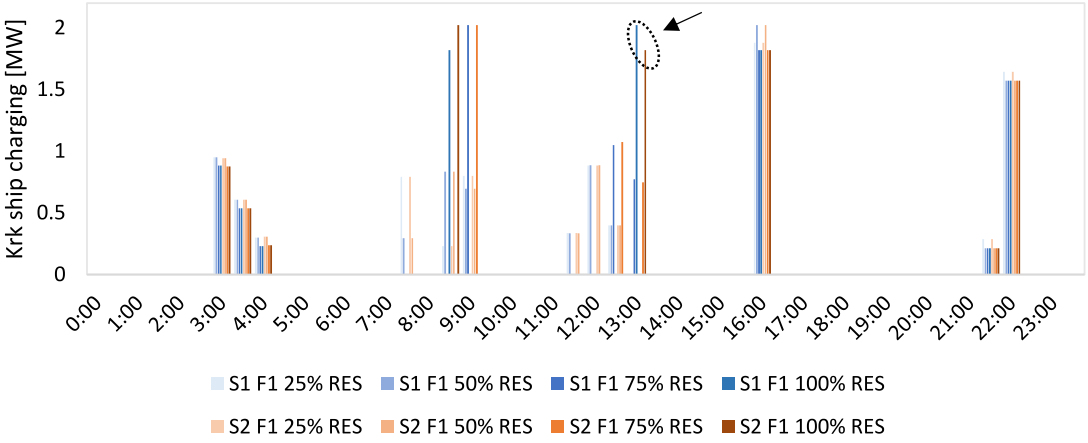

Fig. 9. Krk ship (F1) charging values for scenarios without (S1) and with (S2) the ESS in node 4.

The changes in the charging schedule affect the state of charge of batteries on the ships. The changes between the state of charge of batteries on the ships for 25% and 100% RES are shown in Fig. 11. The results shown in Figs. 9, Figs. 10 and 11 demonstrate the ability of electrified maritime transport to provide flexibility to the observed system. The flexibility provided by maritime transport reduced the amount of curtailed renewable energy and increased the overall social welfare of the observed system.

The ESS operation for the S3 scenario is shown in Fig. 12. The ESS connected at node 4 presents an additional source of flexibility for the

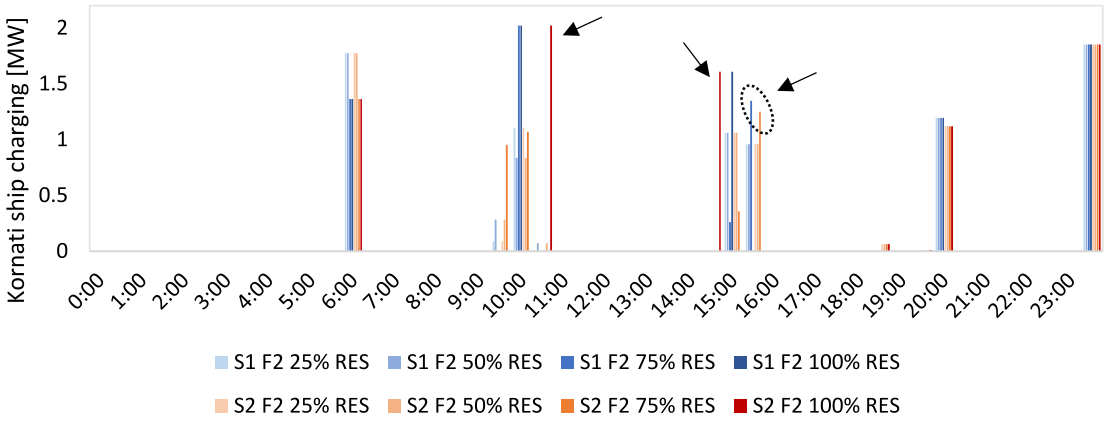

Fig. 10. Kornati ship (F2) charging values for scenarios without (S1) and with (S2) the ESS in node 4.

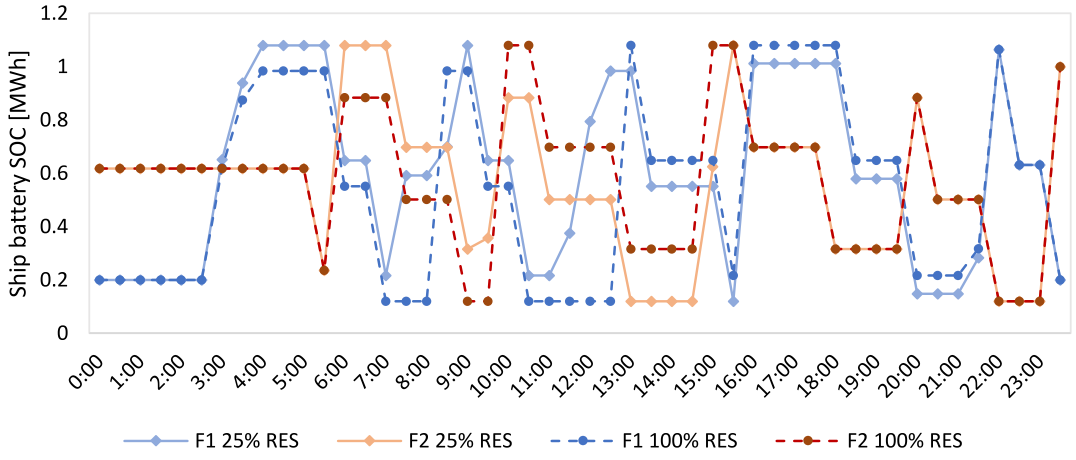

Fig. 11. State of charge of Krk and Kornati batteries for 25% and 100% for the S1 scenario.

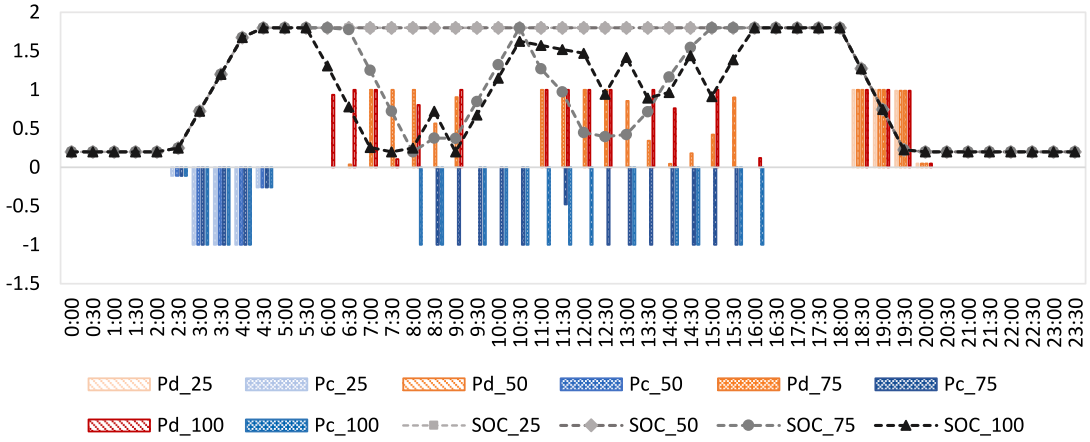

Fig. 12. Battery system operation at node 4 for the S3 scenario for different RES share – charging and discharging (blue and red bars) are expressed in MW and the state of charge of batteries on the ships (lines) are expressed in MWh. (For interpretation of the references to colour in this figure legend, the reader is referred to the Web version of this article.)

system. It can be seen that the operation of the ESS for the 25% and 50% RES share did not change, however, significant differences can be seen for 75% and 100% RES share. The ESS adjusts its operation to reduce the amount of curtailed energy from RES. This means that ESS operation was not determined only by prices of the day ahead electricity market, but also by the curtailed energy. The ESS aimed not only to reduce the amount of curtailed energy but also to reduce it when the market prices were high. Because of this ESS had to discharge at certain periods which caused voltage increase above values that occurred for the S0 scenario (but still below 1.1 pu), which was not the case for the maximum

demand (see Fig. 13).

Moreover, the operation of the ESS was aligned with the charging schedule of the ships. For example, the ESS discharges 1 MW at 9:30 and 10:30 for 75% and 100% RES share and, at the same periods, the Kornati ship was charging (0.95 MW at 9:30 for 75% RES and 2 MW for 100% RES at 10:30). This result implicates that for the large capacity chargers at high RES share, additional sources of flexibility such as ESS reduces the amount of curtailed energy and the operation cost of the system.

The values of the curtailed energy for each scenario and RES share is given in Table 9. The results showed that there was no curtailed energy for the lowest RES share for any scenario. For the 50% RES share, there were low values of curtailed energy for the S0 scenario, while, for the S1 and S2 scenarios, the electric ships and the ESS provided enough flexibility to eliminate curtailed energy.

More significant values of curtailed energy appear for 75% and 100% RES shares. The effect of the flexibility provided by the smart electrification of the maritime transport and connection of the ESS at node 4 can be observed for these high RES cases. The electrification of the maritime transport and its integration with the electric system (the S1 scenario) reduced the amount of curtailed energy by 34.3% (1.92 MWh) in comparison to the base S0 scenario for 75% RES share and 9.8% (2.46 MWh) for 100% RES share. The additional connection of ESS at node 4 reduces the curtailed energy by 55.2% (3.1 MWh) for 75% RES share and 15.7% (3.9 MWh) for the 100% RES share.

As elaborated in the Material and methods section, the proposed AC OPF model enables the calculation of losses in the energy system because $p_{ij} \neq p_{ji}$. The losses for all three scenarios and different RES shares are given in Table 10. It can be seen that the highest increase in losses is achieved for higher RES penetration which was expected because the increase of overall power flow in the grid will lead to higher losses. It is also possible to observe that the charging of the electrical ferry (S1) and the connection of the ESS (S2) did not cause a significant increase in losses. Because there is more curtailed energy for the S0 scenario (lower power flow in the grid) than for S1 and S2, the effect on the losses is even less expressed.

The voltage at node 4 for the minimum demand case is provided in Fig. 13. The results indicate that, for the 25% and 50% RES share, the effect of the maritime transport electrification and additional ESS is similar to the case of maximum demand. The voltage for S1 and S2 was reduced closer to the nominal values, thus the technical grid conditions were improved.

However, differences occur for the 75% and 100% RES share, where the voltage for the S2 scenario raised above the voltage values that occurred for the scenario without maritime electrification (S0). Moreover, the significantly higher voltage reduction values (in comparison to S0 – blue line in Fig. 13) occurred for 75% and 100% RES. These extremes are marked with a dotted black ellipse in Fig. 13. This is connected to the previous results regarding battery storage operation and ship charging schedule. Besides lowering the overall curtailed values, the optimisation algorithm adjusted the charging schedules as well as the ESS operation so that the curtailed values were the lowest for the lowest prices on the day-ahead electricity market. Because of this, increased ship charging values as well as the ESS charging and discharging values during the high PV production caused more frequent voltage deviation. The highest voltage at node 4 was 1.093 pu and, at the same period, the voltage at node 23 reached 1.1 pu. Further increase of voltage at node 4 would cause grid code violation for nodes 22 and 23.

Finally, the energy system operation for the minimum demand case is presented in Fig. 14. The figure shows that the electrification of maritime transport and the installation of the ESS at node 4 had a higher impact on the overall system operation in comparison to the maximum demand case (significant voltage increases and decreases are marked with blue dotted ellipses in Fig. 13).

The presented results showed the benefits of smart cross-sectoral integration, in particular the integration of maritime transport and the electric distribution system. Such integration can improve the technical conditions in the electric grid, enable the higher penetration of RES and increase overall social welfare. The solution where the ESS was connected at the same bus as the electric ship chargers only improved obtained results.

Table 9
Curtailed energy [MWh] for each analysed scenario and different RES share.

RES share/Scenario	S0	S1	S2
25%	0	0	0
50%	0.234	0	0
75%	5.6	3.68	2.51
100%	25.11	22.65	21.18

Table 10
Active losses [MWh] in the observed energy system.

RES share/Scenario	S0	S1	S2
25%	3.72	3.74	3.75
50%	3.82	3.83	3.83
75%	3.81	3.87	3.93
100%	4.43	4.53	4.59

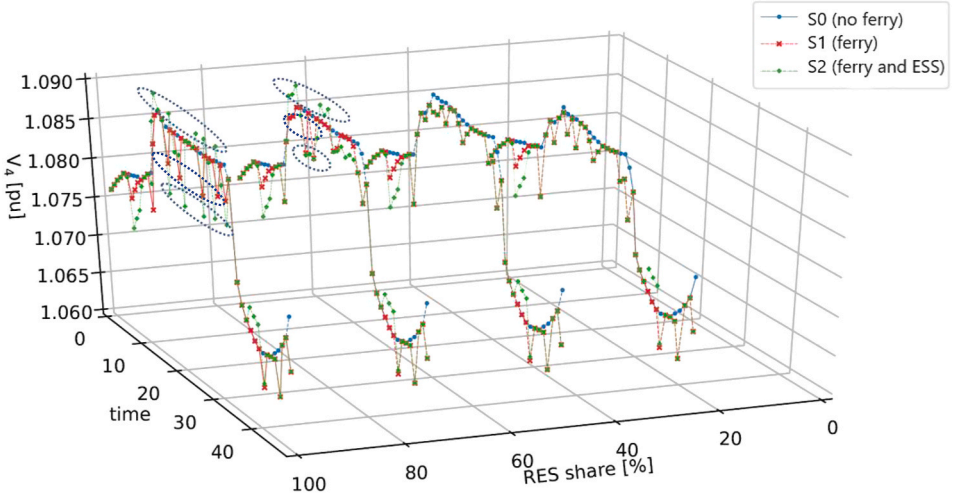

Fig. 13. The voltage at node 4 for minimum demand and all scenarios at different RES share.

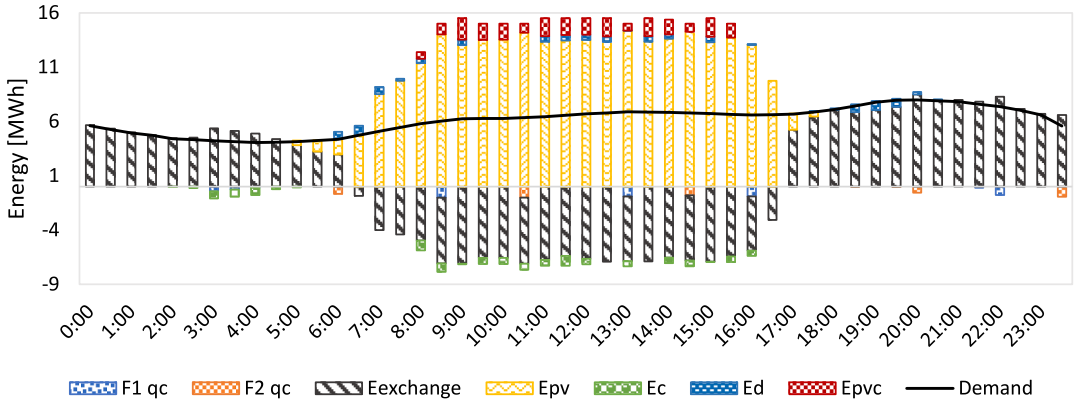

Fig. 14. Energy system operation for scenario S2 for minimum demand case and 100% RES.

5. Discussion

The results of the study indicated that the proposed method and mathematical models can be used for the evaluation of the effects of the integration of the electric distribution grid and maritime transportation into smart energy systems.

The key findings of the study showed that such smart integration improved the technical conditions in the electric grid. The electrification of maritime transport lead to the reduction of the curtailed energy and influenced the electric system operation. The installation of ESS in the electric ferry connection point lead to further reduction of the curtailed energy. Moreover, the results showed that the charging schedule, as well as the ESS operation, changed with respect to the installed RES share. This effect was intensively visible for the high RES share for the minimum demand case. Since the voltage was close to the limits for the minimum demand case, the charging schedule and the ESS operation were adjusted so that the system remained within stable conditions and that the lowest amount of energy was curtailed during periods of high price on the day-ahead electricity market.

To the best of our knowledge, the most relevant study that presented the electric vessel with PV, ESS and grid connection was carried out in Ref. [36]. The authors found that the ESS was mostly charged during the period of low prices in the electricity market. Although this is also true in our study for the maximum demand case, we also found out that the electric ships and the ESS were mostly charged during the peak PV production for the minimum demand scenario. This is the case because the method presented in this paper observed the entire distribution system of the archipelago, which enables to observe the full flexibility potential of maritime and the distribution system integration. This proved to be especially important for the periods when the system is close to the limits prescribed by the grid code limitations, which was not discussed in Ref. [36].

The detailed distribution system modelled in this study realistically captured the possible voltage violations and congestions. The application of such a detailed distribution system model, in combination with the presented electrical ferry model, enabled us to observe the impacts of smart integration of the maritime and electricity sector during both, the normal and disturbed operating parameters of the distributions system. A similar model was previously used in Ref. [37] for assessing the impact of the price-sensitive top-down demand response model. The model in Ref. [37] considered a smaller distribution system around Lošinj island and a maximum installed RES capacity of 20.5 MW. The maximum reduction of the curtailed energy was 3.5% lower for the scenario with demand response in comparison to the base scenario. This study considered a larger system around Krk island and considered a maximum of 30 MW RES installed. The maximum reduction of curtailed energy as a result of maritime electrification (S1) in this paper was 9.8% in comparison to base scenario S0. This means that the presented cross-sector integration had a larger impact than the price responsive demand response model. However, this was expected because the capacity of ship charging stations was approximately two times higher than the used price responsive demand response. Additionally, the charging stations were connected to one bus in the system which enabled a stronger local impact on the technical parameters of the observed system. The proposed model can also be used as a basis for further sector coupling and the creation of smart energy systems such as water and energy systems as in Ref. [38], or land transport integration as in Ref. [39].

The case study in this paper used the PV curve that represents the maximum daily PV production for both cases – maximum and minimum demand. Since the maximum demand is achieved during the summer period and the minimum demand is usually for the winter or autumn period, one could argue that a different PV curve that represents the average or minimum production should be used for the minimum demand case. Although it is reasonable to question this, there are at least two reasons why this should be avoided. First, the aim of the study is to demonstrate the effects of smart cross-sector integration for marginal system operation in high RES surrounding to observe the full effect of newly introduced flexibility in the system. Since the highest voltage will appear for the minimum demand and the highest generation, this scenario should be considered. Moreover, at least two technical studies ([33,40]) showed that maximum PV production can also occur during potential periods of minimum demand for the observed location, thus further underlining the necessity to analyse such a scenario. The second argument is that all of the results of the study were presented with respect to the different RES shares. Thus, the cases for lower PV production were analysed for 25% and 50% RES scenarios, which is considered enough to show the effects of lower PV production during minimum demand. The results were in accordance with the statements made in this chapter – that the most interesting case is for the highest RES production and the minimum demand. Thus, it can be concluded that the conducted sensitivity analysis well represents the system behaviour for different cases and that the minimum demand and 100% RES scenario fully demonstrate the possible exploitation of the flexibility potential of maritime electrification.

Although this study did propose a model that considered the ship battery energy loss when the ship is not sailing, the study did not include a battery degradation effect and this imposes a limit on this study. The degradation effect can have a long-term impact on the operation of the electric ships and should be investigated. However, in our study, it is acceptable to neglect this effect because this study aims at investigating the effects of cross-sector integration of maritime transport with the electrical grid, with a particular emphasis on the technical impacts on the power system grid. Moreover, since the variables and parameters

used in the proposed approach are general and can be applied to any distribution system or electric ship, the proposed method can be applied to numerous case studies. It can be expected that similar results and conclusions would be achieved for other case studies, however, the precise impact will differ from one site to another and the proposed approach enables the quantification of these impacts for each site.

The presented study implicates the need to accelerate the creation of the financial and regulatory frameworks that will stimulate the smart electrification of maritime transport. In order to achieve the integration, it will be necessary to build the proper infrastructure and smart ports [41]. This will lead towards the increased penetration of RES in the energy systems and contribute to further sector coupling and energy transition.

6. Conclusion

This study presented a novel approach for the assessment of smart integration of the electrified maritime transport sector with the electric power system sector. The method proposed a mathematical model for the electric ships integrated into the detailed distribution system. The case study was conducted on the example of the Kvarner archipelago with the aim of observing the effects of cross-sector integration under the different penetration of renewable energy sources. The results of the study showed that:

- The cross-sector integration of maritime transport and electric power system with installed energy storage system resulted in the decrease of curtailed energy for 3.9 MWh when 30 MW on installed photovoltaics were installed in the grid in comparison to the case without the electrified maritime transport
- The integration of electrified maritime transport improved the voltage conditions during the maximum demand in the archipelago. The voltage at the ferry connection node reduced up to 0.845 kV when the ferries were connected in order to decrease the amount of the curtailed energy
- The charging schedule of the electric ships changed with the increased share of renewable energy sources while maintaining the passenger transport timeline. The changes went up to 2 MW of increased charging for the highest share of renewable energy sources present in the system
- The results of the study indicate the need for the creation of the supporting schemes and frameworks that will stimulate the electrification of maritime transport and its integration with the electric power system

The future research will be oriented towards the investigation of different possibilities of maritime transport electrification with an emphasis on their market integration. This will be done through the application of different incentives and support to electrified maritime transport.

Declaration of competing interest

The authors declare that they have no known competing financial interests or personal relationships that could have appeared to influence the work reported in this paper.

Acknowledgement

This work has been supported by the Young Researchers' Career Development Programme (DOK-01-2018) of Croatian Science Foundation which is financed by the European Union from European Social Fund and Horizon 2020 project INSULAE - Maximizing the impact of innovative energy approaches in the EU islands (Grant number ID: 824433). This support is gratefully acknowledged.

References

[1] International Maritime Organization. Fourth IMO GHG study-executive summary. 2020.
[2] DNV, "Energy efficiency existing ship index (EEXI)." .
[3] DNV, "Achieving the IMO decarbonization goals." .
[4] Korberg AD, Brynolf S, Grahn M, Skov IR. Techno-economic assessment of advanced fuels and propulsion systems in future fossil-free ships. Renew Sustain Energy Rev May 2021;142:110861.
[5] Sterling PlanB Energy Solutions (SPBES), "Electrification of ships." .
[6] Nuchturee C, Li T, Xia H. Energy efficiency of integrated electric propulsion for ships – a review. Renew Sustain Energy Rev Dec. 2020;134:110145.
[7] DNV GL AS Maritime. Electrical energy storage for ships. 2020.
[8] Gagatsi E, Estrup T, Halatsis A. Exploring the potentials of electrical waterborne transport in europe: the E-ferry concept. Transport Res Procedia 2016;14:1571–80.
[9] Tvedten IØ, Bauer S. Retrofitting towards a greener marine shipping future: reassembling ship fuels and liquefied natural gas in Norway. Energy Res Social Sci Apr. 2022;86:102423.
[10] Wang L, Hu J, Yu Y, Huang K, Hu Y. Lithium-air, lithium-sulfur, and sodium-ion, which secondary battery category is more environmentally friendly and promising based on footprint family indicators? J Clean Prod Dec. 2020;276:124244.
[11] Blanco-Davis E, Zhou P. LCA as a tool to aid in the selection of retrofitting alternatives. Ocean Eng Feb. 2014;77:33–41.
[12] Perčić M, Vladimir N, Fan A. Techno-economic assessment of alternative marine fuels for inland shipping in Croatia. Renew Sustain Energy Rev Sep. 2021;148:111363.
[13] Perčić M, Vladimir N, Fan A. Life-cycle cost assessment of alternative marine fuels to reduce the carbon footprint in short-sea shipping: a case study of Croatia. Appl Energy Dec. 2020;279:115848.
[14] Wang H, Boulougouris E, Theotokatos G, Zhou P, Priftis A, Shi G. Life cycle analysis and cost assessment of a battery powered ferry. Ocean Eng Dec. 2021;241:110029.
[15] Dominković DF, Weinand JM, Scheller F, D'Andrea M, McKenna R. Reviewing two decades of energy system analysis with bibliometrics. Renew Sustain Energy Rev Jan. 2022;153:111749.
[16] Scheller F, Wiese F, Weinand JM, Dominković DF, McKenna R. An expert survey to assess the current status and future challenges of energy system analysis. Smart Energy Nov. 2021;4:100057.
[17] Marczinkowski HM, Barros L. Technical approaches and institutional alignment to 100% renewable energy system transition of madeira island-electrification, smart energy and the required flexible market conditions. Energies 2020;13(17).
[18] Duić N, Krajačić G, da Graça Carvalho M. RenewIslands methodology for sustainable energy and resource planning for islands. Renewable and Sustainable Energy Reviews; 2008.
[19] Matamala Y, Feijoo F. A two-stage stochastic Stackelberg model for microgrid operation with chance constraints for renewable energy generation uncertainty. App Energy 2021;303. https://doi.org/10.1016/j.apenergy.2021.117608.
[20] Mimica M, Giménez de Urtasun L, Krajačić G. A robust risk assessment method for energy planning scenarios on smart islands under the demand uncertainty. Energy Feb. 2022;240:122769.
[21] Martorana F, Giardina M, Buffa P, Beccali M, Zammuto C. A new tool to process forecast meteorological data for atmospheric pollution dispersion simulations of accident scenarios: a sicily-based case study. J. Sustain. Dev. Energy, Water Environ. Syst. 2021;9(3).
[22] Groppi D, Pfeifer A, Garcia DA, Krajačić G, Duić N. A review on energy storage and demand side management solutions in smart energy islands. Renew Sustain Energy Rev 2021;135. https://doi.org/10.1016/j.rser.2020.110183.
[23] Hao H, Huang B, Ji P. Optimal Configuration of An Island Microgrid Considering Demand Response Strategy 2021;36:300–4.
[24] Mimica M, Krajačić G. The Smart Islands method for defining energy planning scenarios on islands. Energy 2021;237.
[25] Curto D, Franzitta V, Trapanese M, Cirrincione M. A preliminary energy assessment to improve the energy sustainability in the small islands of the mediterranean sea. N/A J. Sustain. Dev. Energy, Water Environ. Syst. 2020 N/A.
[26] Agathokleous RA, Kalogirou SA. PV roofs as the first step towards 100% RES electricity production for Mediterranean islands: the case of Cyprus. Smart Energy Nov. 2021;4:100053.
[27] Ocon JD, Bertheau P. Energy transition from diesel-based to solar photovoltaics-battery-diesel hybrid system-based island grids in the Philippines – techno-economic potential and policy implication on missionary electrification. J. Sustain. Dev. Energy, Water Environ. Syst. 2019;7(1).
[28] Dominkovic DF, Stark G, Hodge BM, Pedersen AS. Integrated energy planning with a high share of variable renewable energy sources for a Caribbean Island. 2018. Energies.
[29] Adland R, Cariou P, Wolff FC. Optimal ship speed and the cubic law revisited: empirical evidence from an oil tanker fleet. Transport Res Part E Logist Transp Rev Aug. 2020;140:101972.
[30] Jadrolinija, "Ferry lines schedule." .
[31] Croatian Register of Shipping, "Web report of a ship." .
[32] Mimica M, Dominković DF, Kirinčić V, Krajačić G. Soft-linking of improved spatiotemporal capacity expansion model with a power flow analysis for increased integration of renewable energy sources into interconnected archipelago. Appl Energy Jan. 2022;305:117855.
[33] Cerovečki T, Cvitanović M, Damjanović F, Ivković R, Majcen J, Širić I. Optimal technical connection of PV plant on distribution grid. 2019.
[34] www.cropex.hr.

[35] Kumar J, Memon AA, Kumpulainen L, Kauhaniemi K, Palizban O. Design and analysis of new harbour grid models to facilitate multiple scenarios of battery charging and onshore supply for modern vessels. Energies 2019;12(12).
[36] Hein K, Yan X, Wilson G. Multi-objective optimal scheduling of a hybrid ferry with shore-to-ship power supply considering energy storage degradation. Electron 2020; 9(5).
[37] Mimica M, Dominković DF, Capuder T, Krajačić G. On the value and potential of demand response in the smart island archipelago. Renew Energy 2021;176. https://doi.org/10.1016/j.renene.2021.05.043.
[38] Assareh E, Delpisheh M, Alirahmi SM, Tafi S, Carvalho M. Thermodynamic-economic optimization of a solar-powered combined energy system with desalination for electricity and freshwater production. Smart Energy; Dec. 2021, 100062.
[39] Boström T, Babar B, Hansen JB, Good C. The pure PV-EV energy system – a conceptual study of a nationwide energy system based solely on photovoltaics and electric vehicles. Smart Energy Feb. 2021;1:100001.
[40] RINA-C. Insulae - energy storage system - conceptual design Unije. 2019.
[41] Kumar J, Khan HS, Kauhaniemi K. Smart control of battery energy storage system in harbour area smart grid: a case study of vaasa harbour. In: EUROCON 2021 - 19th IEEE international conference on smart technologies, proceedings; 2021.